

Supporting Information for Copolymerization of CHO/CO₂ catalyzed by a series of aluminum amino-phenolate complexes and insights into structure-activity relationships

Hart Plommer,^{a,b} Laura Stein,^a Jennifer N. Murphy,^a Nduka Ikpo,^a Nelaine Mora-Diez,^b and Francesca M. Kerton^{*a}

- a) Department of Chemistry, Memorial University of Newfoundland, St. John's, NL, A1B 3X7, Canada
b) Department of Chemistry, Thompson Rivers University, Kamloops, BC, V2C 0C8, Canada

Figure S1. Molecular structure and partial numbering of 2 (thermal ellipsoids drawn at 50% probability; H atoms and two co-crystallized toluene molecules excluded for clarity). Selected bond distances (Å) and angles (°): Cl(1)–Al(1), 2.2532(13); Al(1)–O(1), 1.752(3); Al(1)–O(2), 1.745(3); Al(1)–N(1), 2.069(3); Al(1)–N(2), 2.116(3); O(1)–Al(1)–Cl(1), 93.88(9); O(1)–Al(1)–N(1), 113.11(12); O(1)–Al(1)–N(2), 91.21(12); O(2)–Al(1)–Cl(1), 91.05(9); O(2)–Al(1)–O(1), 124.52(13); O(2)–Al(1)–N(1), 122.09(13); O(2)–Al(1)–N(2), 90.72(12); N(1)–Al(1)–Cl(1), 90.40(9); N(1)–Al(1)–N(2), 82.40(12); N(2)–Al(1)–Cl(1), 172.39(10).....	4
Figure S2. ¹ H NMR spectrum of H[L2] in CDCl ₃ , 298 K.....	5
Figure S3. ¹³ C { ¹ H} NMR spectrum of H[L2] in CDCl ₃ , 298 K.....	6
Figure S4. ¹ H NMR spectrum of 2 in CDCl ₃ , 298 K.....	7
Figure S5. HSQC spectrum of 2 in CDCl ₃ , 298 K	8
Figure S6. ¹³ C-DEPT NMR spectrum of 2 in CDCl ₃ , 298 K.....	9
Figure S7. ¹ H NMR spectrum of 3 in CDCl ₃ , 298 K (residual toluene resonance at 2.36 ppm)	10
Figure S8. ¹³ C-DEPT NMR spectrum of 3 in CDCl ₃ , 298 K.....	11
Figure S9. COSY spectrum of 3 in CDCl ₃ , 298 K	12
Figure S10. HSQC spectrum of 3 in CDCl ₃ , 298 K	13
Figure S11. ¹³ C spectrum of 4 in CDCl ₃ , 298 K.....	14
Figure S12. HSQC spectrum of 4 in CDCl ₃ , 298 K	15
Figure S13. ¹ H NMR spectrum of 5 in CDCl ₃ , 298 K (residual toluene resonance at 2.41 ppm)	16
Figure S14. ¹³ C NMR spectrum of 5 in CDCl ₃ , 298 K	17
Figure S15. HSQC spectrum of 5 in CDCl ₃ , 298 K	18
Figure S16. Monitoring of IR absorptions over time at variable temperatures for the reaction of 1+PPNCl+CHO (1/1/500) at 40 bar CO ₂ . Red (1800 cm ⁻¹ , CHC formation) and green (1750 cm ⁻¹ , PCHC formation). Note: Under ideal circumstances, individual and replicant reactions should be performed at each temperature.	19
Figure S17. MALDI-TOF mass spectrum of H[L2]	20
Figure S18. MALDI-TOF MS spectra of 2	21
Figure S19. MALDI-TOF mass spectra of 4.3 (experimental – top, theoretical – bottom)	22

Figure S20. Representative GPC trace of isolated PCHC (Table 1, entry 6; the peaks around 80 min are due to the delay volume)	23
Figure S21. Possible catalytic mechanisms for ROCOP mediated by Al complexes	27

Table S1. Crystallographic and structure refinement data for compounds H[L2], 2 , 4 , and 5	3
Table S2. Experimental (X-ray) and calculated (M06/6-311+G(d,p)) bond distances of 1 , 2 , 4 , and 5	24
Table S3. Calculated charges of pendent nitrogen in initial pro-ligands and Al-Cl complexes...25	
Table S4. Calculated (M06/6-311+G(d,p)) Al charges and relevant bond distances of Al-carbonate derivatives	25
Table S5. Highly active catalyst systems for copolymerization of CHO/CO ₂	26

Table S1. Crystallographic and structure refinement data for compounds H[L2], **2**, **4**, and **5**

Compounds	H[L2]	2	4	5
Chemical formula	C ₂₁ H ₃₅ NO ₂	C ₄₈ H ₇₀ AlClN ₂ O ₂	C ₄₂ H ₆₈ N ₂ O ₂ AlCl	C ₇₅ H ₁₁₁ Al ₂ Cl ₂ N ₄ O ₄
Formula weight	333.51	769.49	695.41	1257.53
Temperature/K	123	100	293(2)	100
Crystal system	monoclinic	monoclinic	triclinic	triclinic
Space group	P2 ₁ /c	P2 ₁ /n	P-1	P-1
a/Å	12.013(4)	13.1378(4)	11.4893(3)	7.7750(2)
b/Å	17.863(6)	24.9763(6)	13.7084(4)	11.1513(3)
c/Å	9.836(3)	14.4263(4)	15.1276(3)	21.4322(5)
$\alpha/^\circ$	90	90	111.101(2)	75.708(2)
$\beta/^\circ$	101.484(5)	110.413(3)	105.252(2)	89.494(2)
$\gamma/^\circ$	90	90	93.044(2)	74.480(2)
Volume/Å ³	2068.5(12)	4436.5(2)	2115.43(10)	1731.77(8)
Z	4	4	2	1
$D_c/\text{g cm}^{-3}$	1.071	1.152	1.092	1.206
Radiation type	MoKα ($\lambda = 0.71075$)	MoKα ($\lambda = 0.71073$)	MoKα ($\lambda = 0.71073$)	MoKα ($\lambda = 0.71073$)
μ (MoKα)/mm ⁻¹	0.067	0.145	0.145	0.171
F(000)	736	1672.0	760.0	681.0
Reflections measured	21073	56957	27634	22667
Unique reflections	4291	8121	8009	6588
R_{int}	0.0239	0.1011	0.0425	0.0403
R_I (all)	0.0529	0.1157	0.0604	0.0675
$wR(F^2)$ (all)	0.1276	0.1875	0.1249	0.1563
R_I ($I > 2 \sigma(I)$) ^a	0.0497	0.0981	0.0491	0.0598
$wR(F^2)$ ($I > 2 \sigma(I)$) ^b	—	0.1769	0.1161	0.1499
Goodness of fit on F^2	1.112	1.181	1.058	1.086
CCDC Ref.	1912327	1936692	1936648	1936691

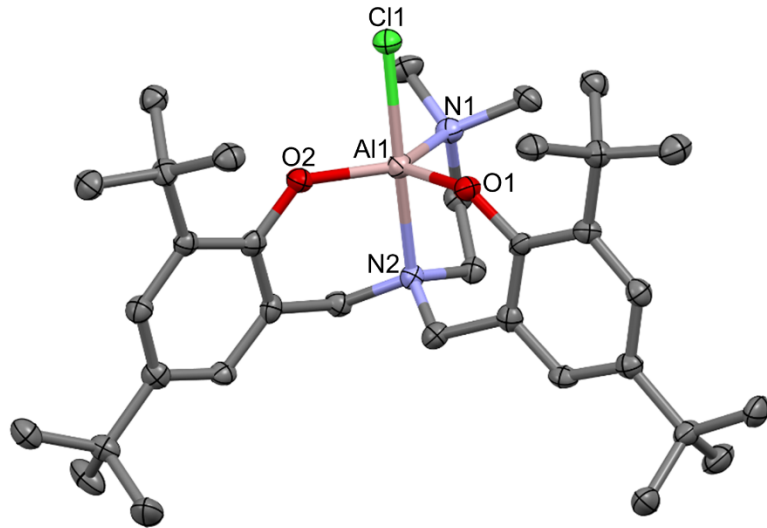
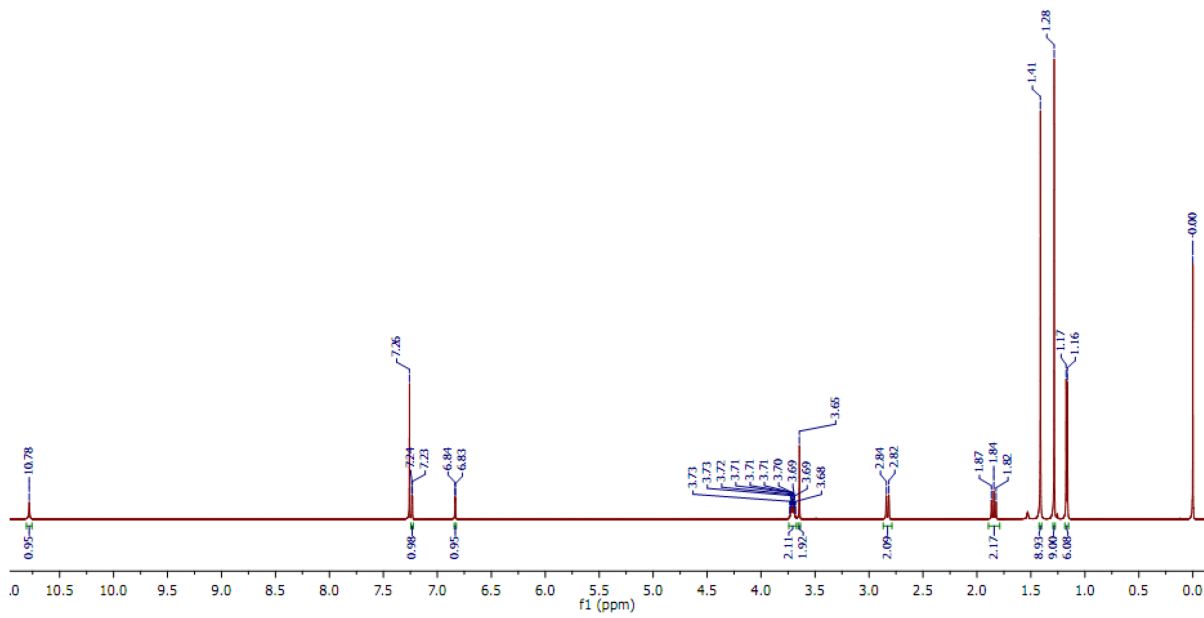


Figure S1. Molecular structure and partial numbering of **2** (thermal ellipsoids drawn at 50% probability; H atoms and two co-crystallized toluene molecules excluded for clarity). Selected bond distances (\AA) and angles ($^\circ$): Cl(1)–Al(1), 2.2532(13); Al(1)–O(1), 1.752(3); Al(1)–O(2), 1.745(3); Al(1)–N(1), 2.069(3); Al(1)–N(2), 2.116(3); O(1)–Al(1)–Cl(1), 93.88(9); O(1)–Al(1)–N(1), 113.11(12); O(1)–Al(1)–N(2), 91.21(12); O(2)–Al(1)–Cl(1), 91.05(9); O(2)–Al(1)–O(1), 124.52(13); O(2)–Al(1)–N(1), 122.09(13); O(2)–Al(1)–N(2), 90.72(12); N(1)–Al(1)–Cl(1), 90.40(9); N(1)–Al(1)–N(2), 82.40(12); N(2)–Al(1)–Cl(1), 172.39(10).



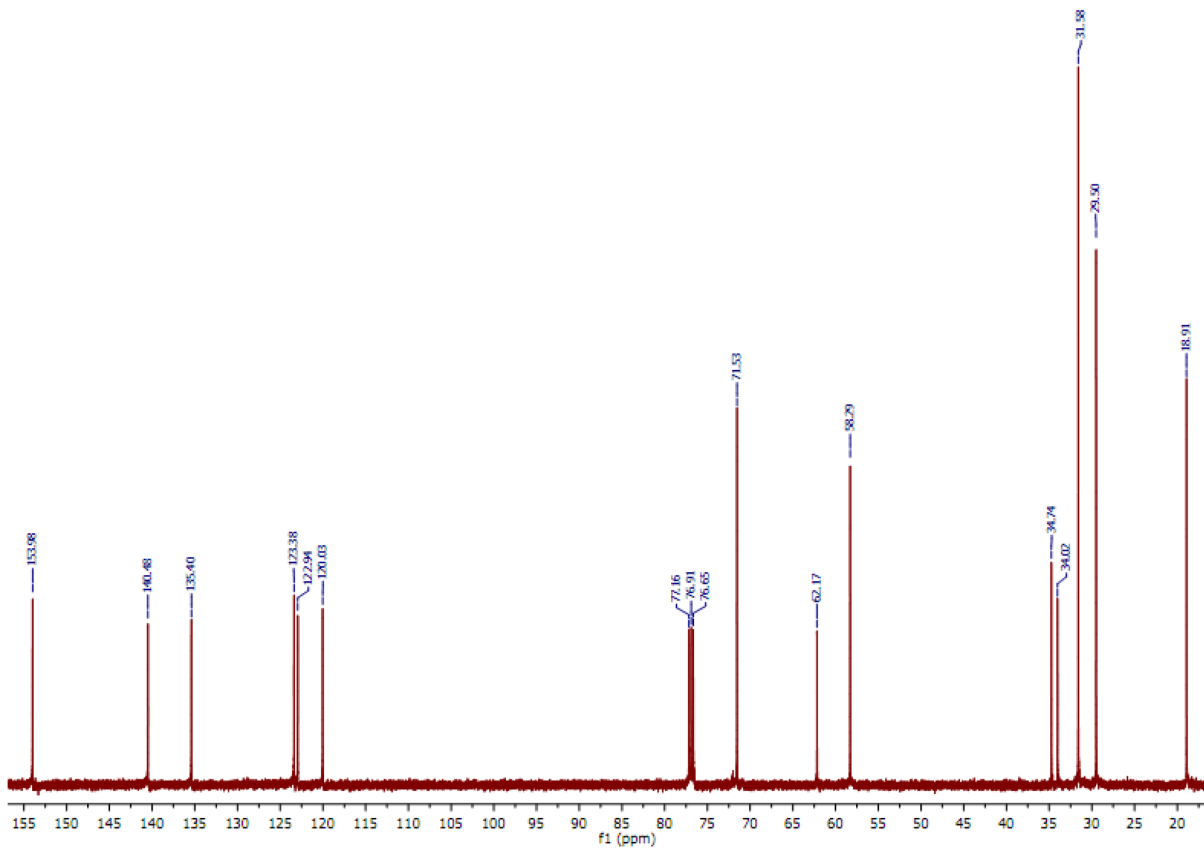


Figure S3. ^{13}C $\{^1\text{H}\}$ NMR spectrum of H[L2] in CDCl_3 , 298 K

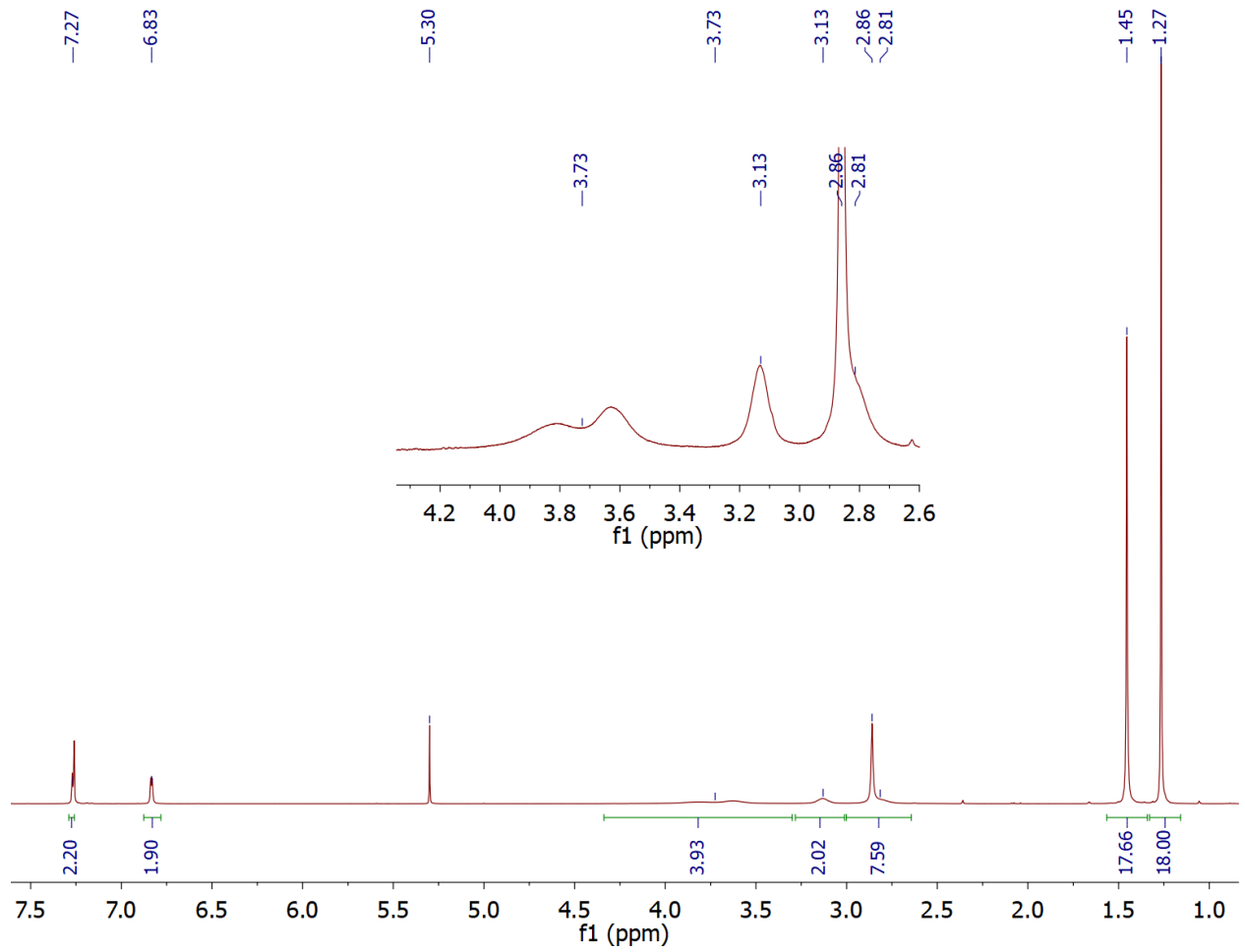


Figure S4. ${}^1\text{H}$ NMR spectrum of **2** in CDCl_3 , 298 K

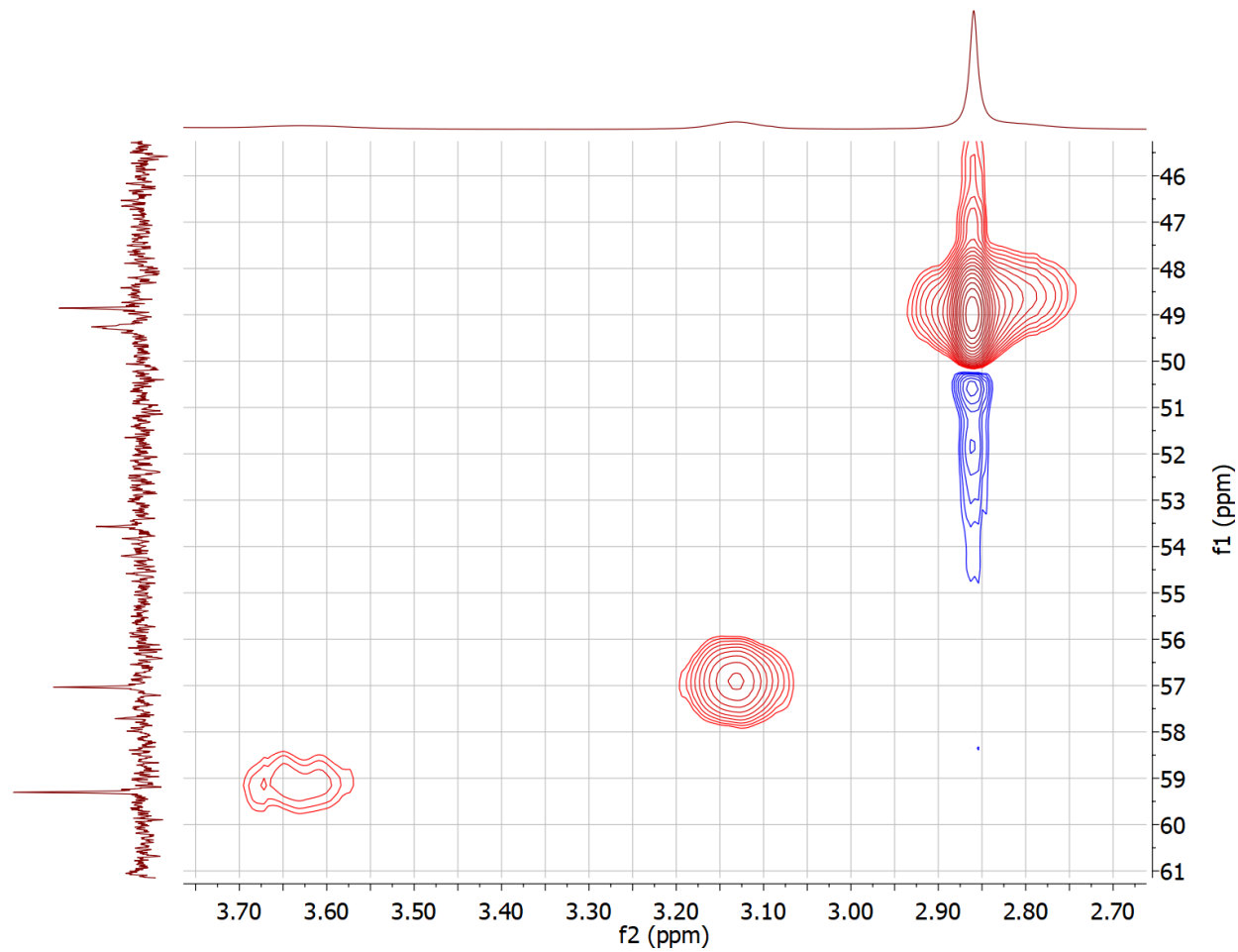


Figure S5. HSQC spectrum of **2** in CDCl_3 , 298 K

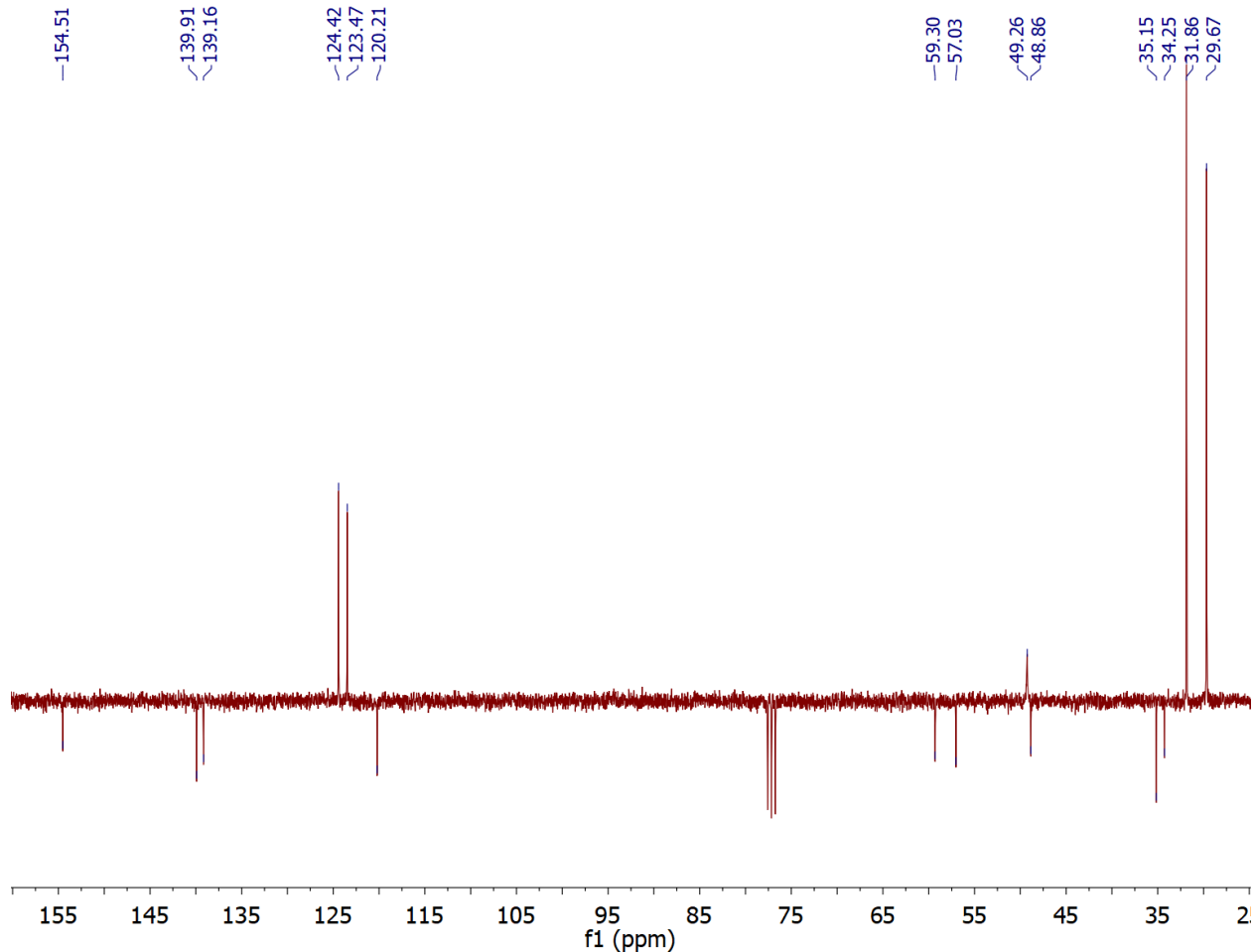


Figure S6. ¹³C-DEPT NMR spectrum of **2** in CDCl_3 , 298 K

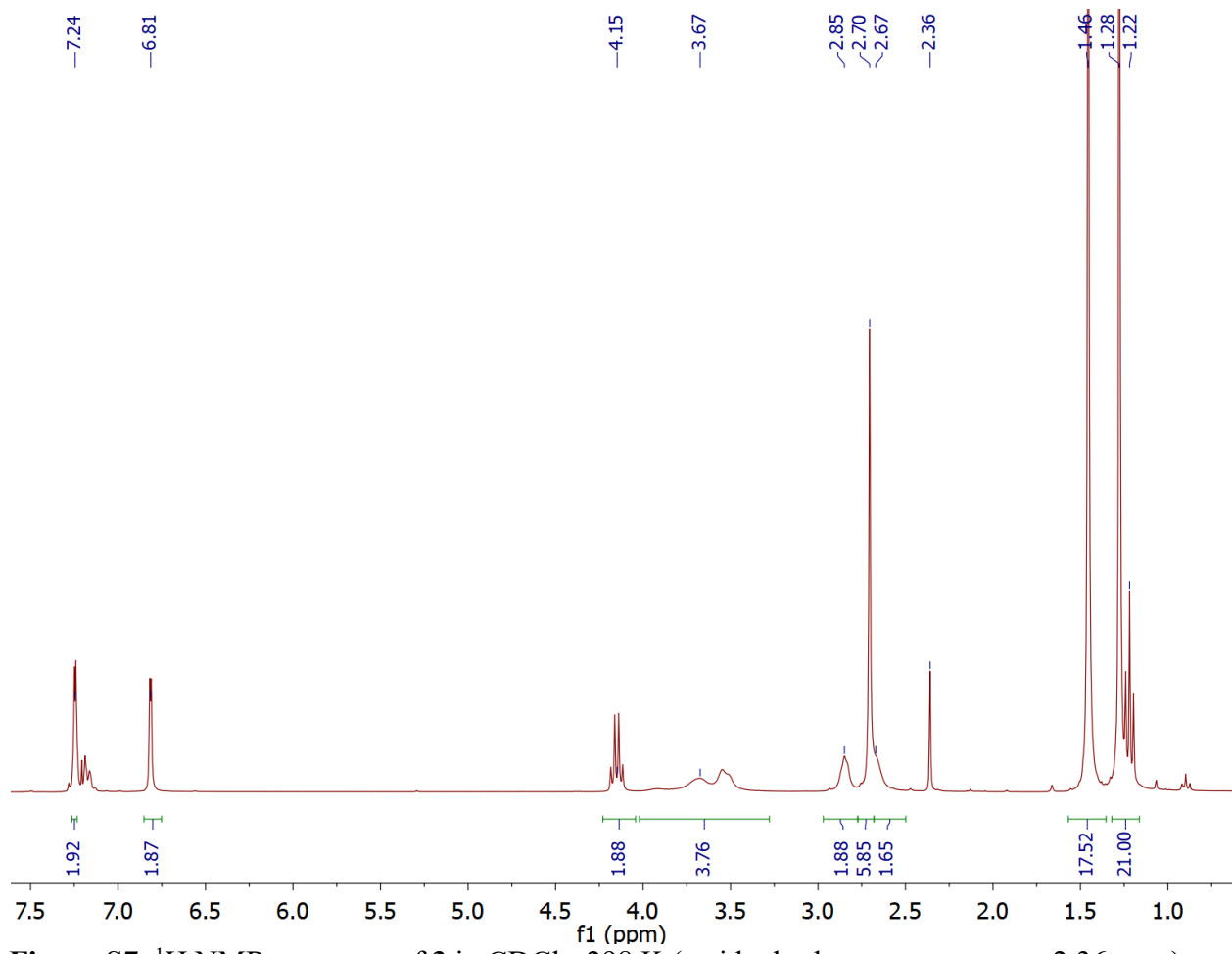


Figure S7. ${}^1\text{H}$ NMR spectrum of **3** in CDCl_3 , 298 K (residual toluene resonance at 2.36 ppm)

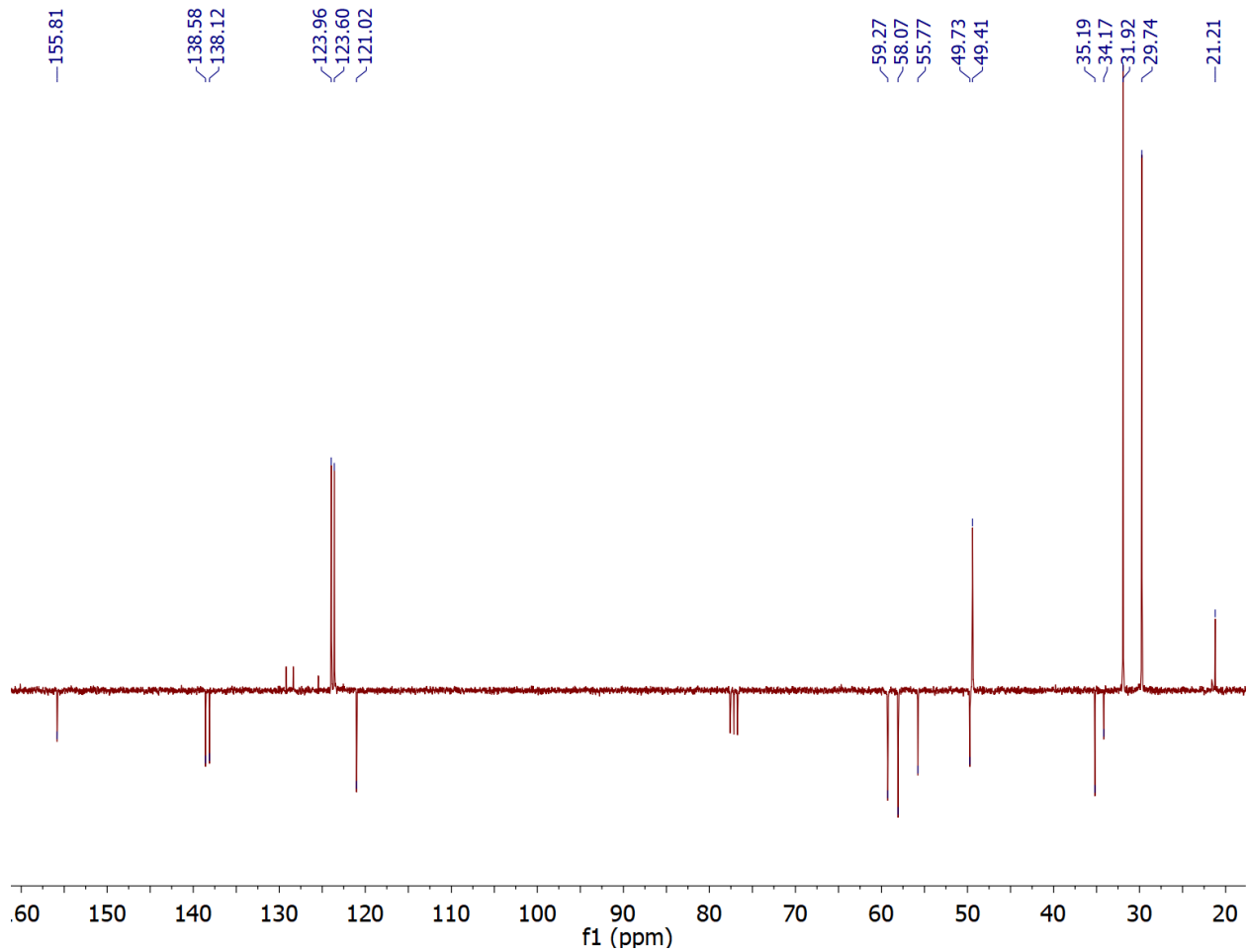


Figure S8. ^{13}C -DEPT NMR spectrum of **3** in CDCl_3 , 298 K

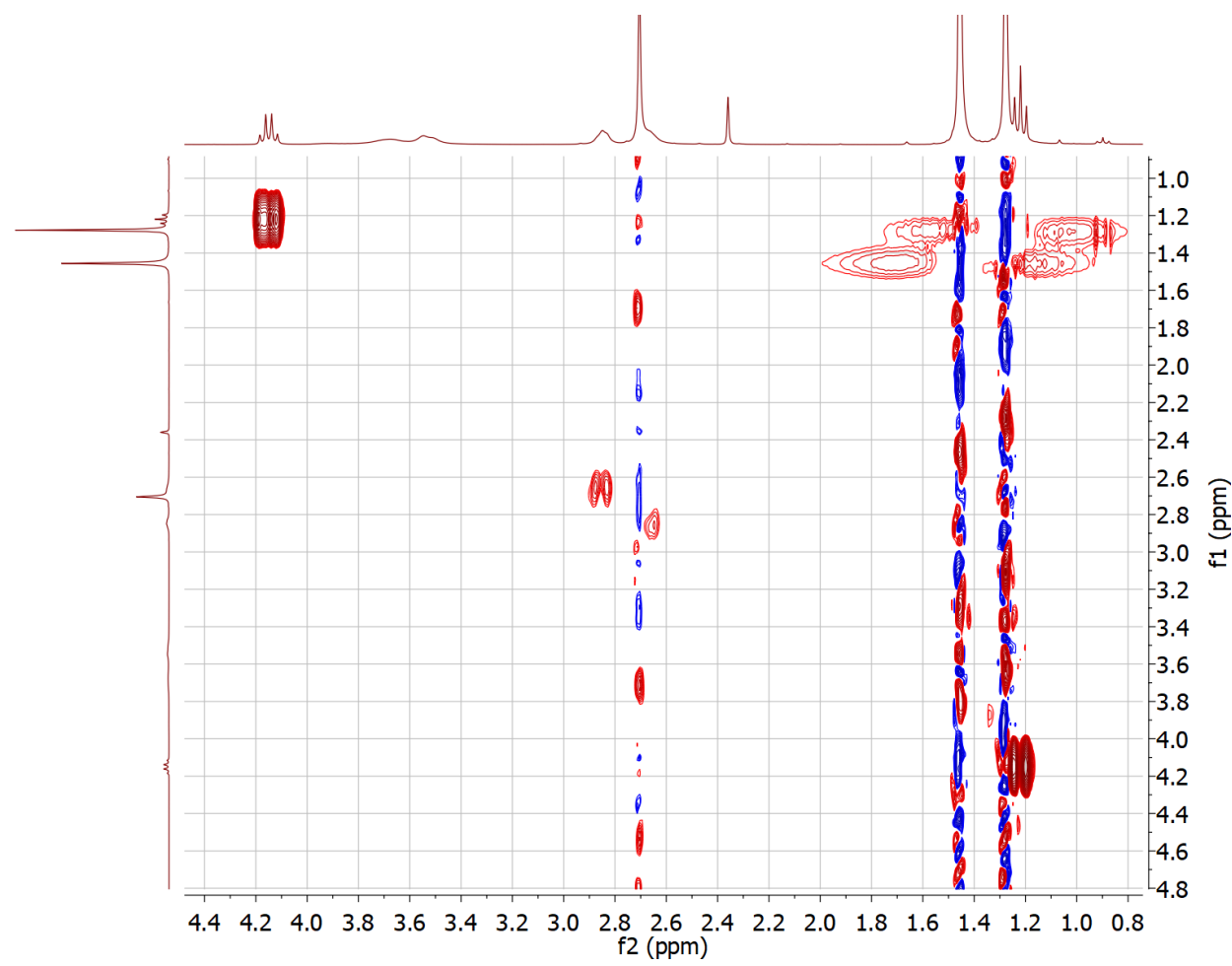


Figure S9. COSY spectrum of **3** in CDCl_3 , 298 K

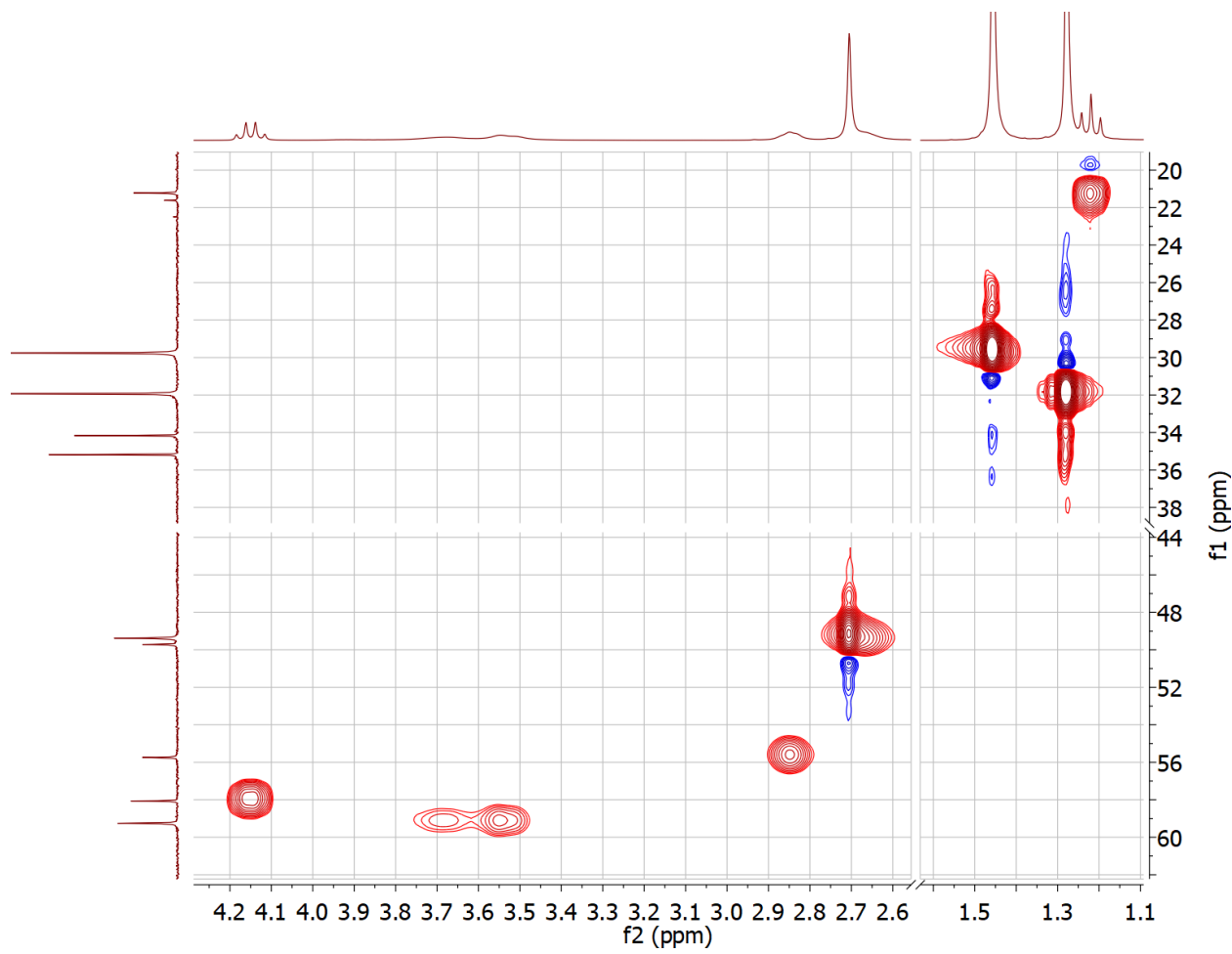


Figure S10. HSQC spectrum of **3** in CDCl_3 , 298 K

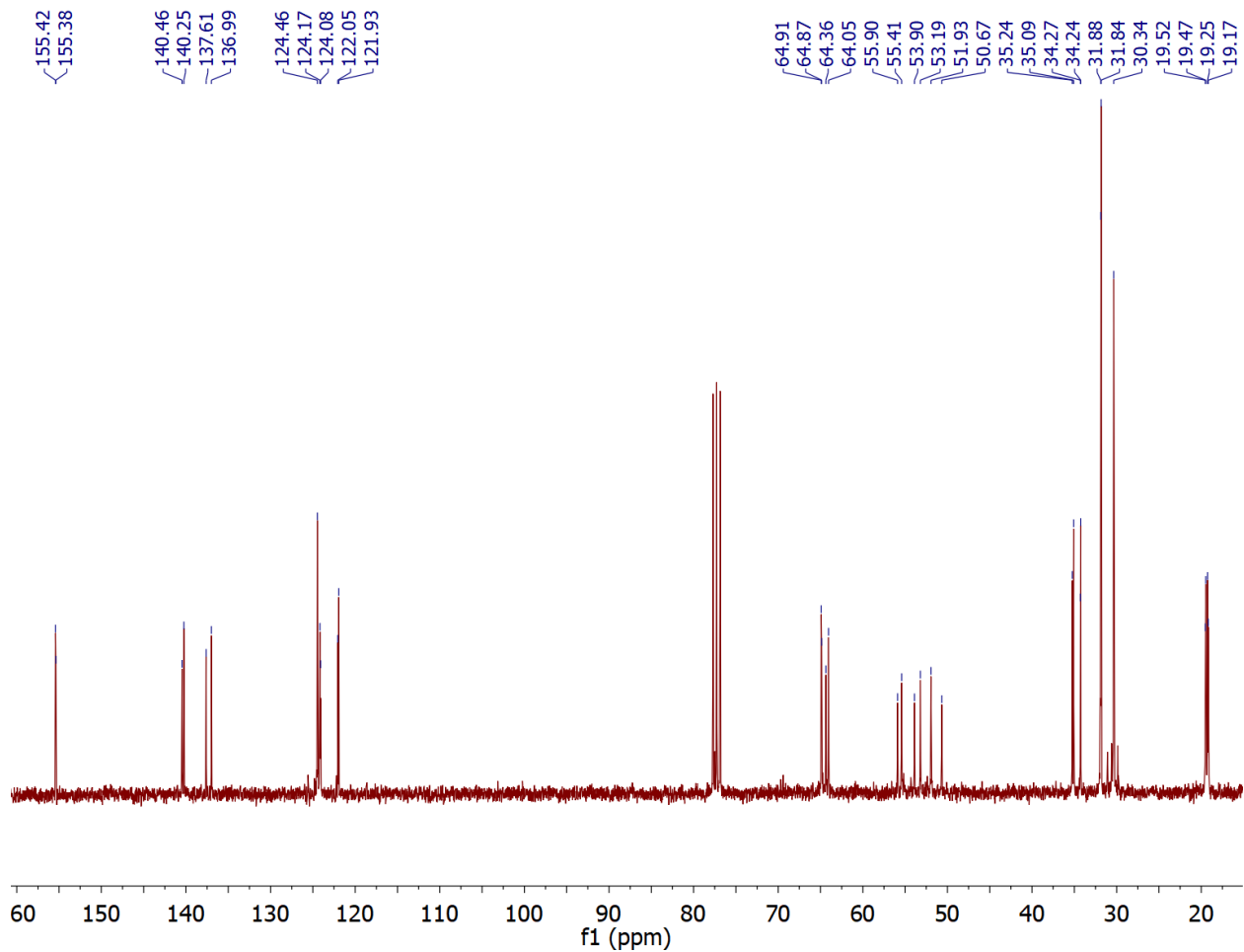


Figure S11. ^{13}C spectrum of **4** in CDCl_3 , 298 K

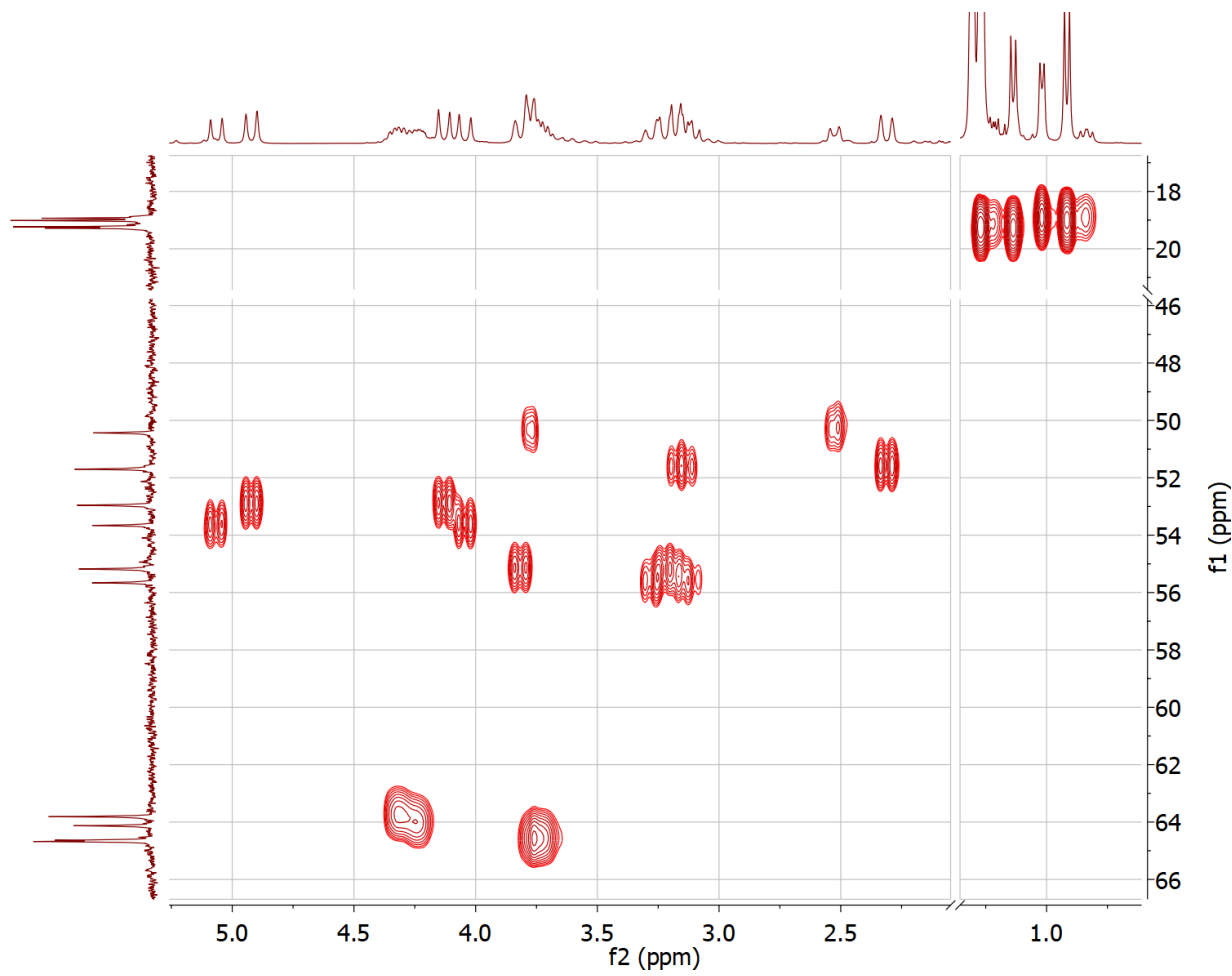


Figure S12. HSQC spectrum of **4** in CDCl_3 , 298 K

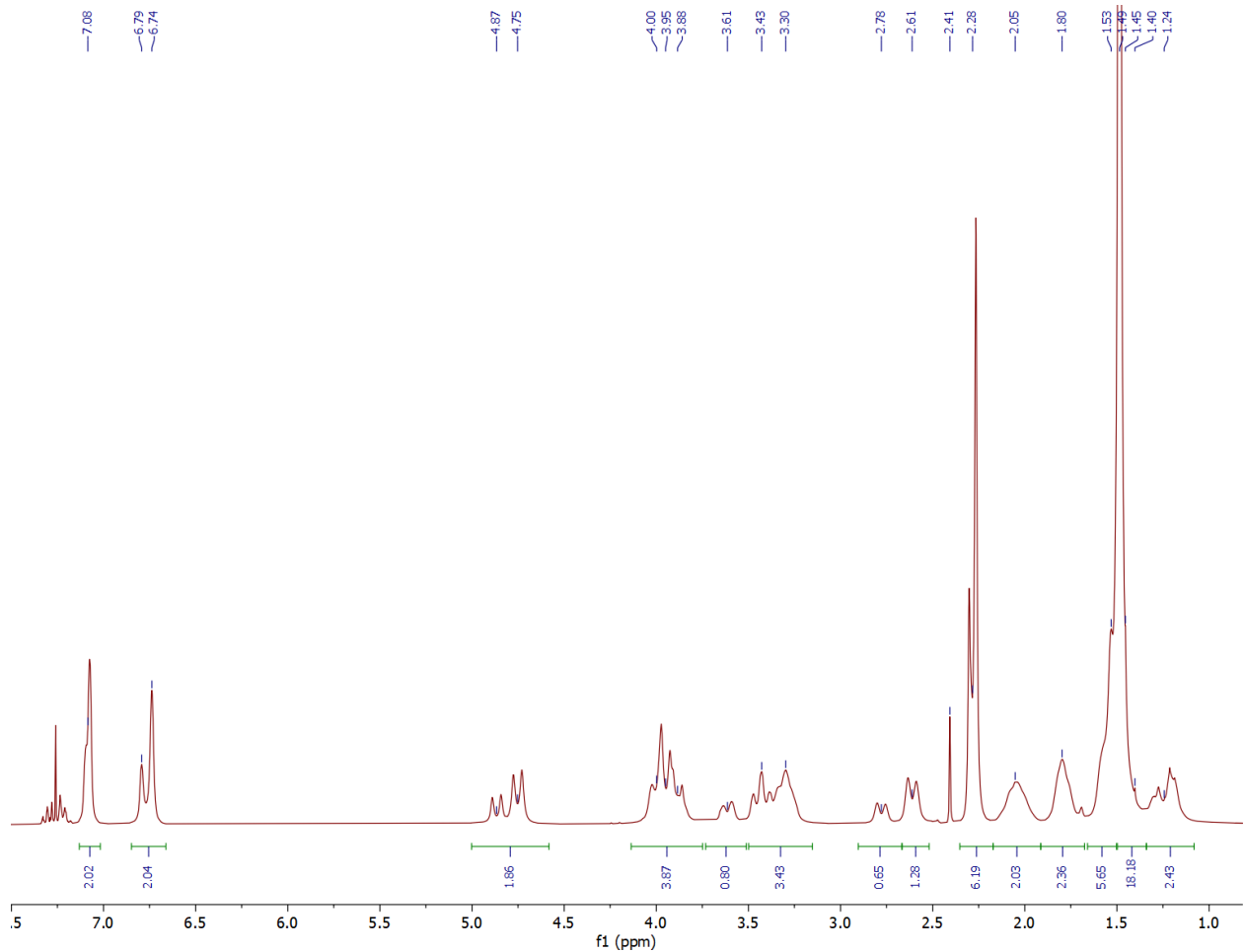


Figure S13. ^1H NMR spectrum of **5** in CDCl_3 , 298 K (residual toluene resonance at 2.41 ppm)

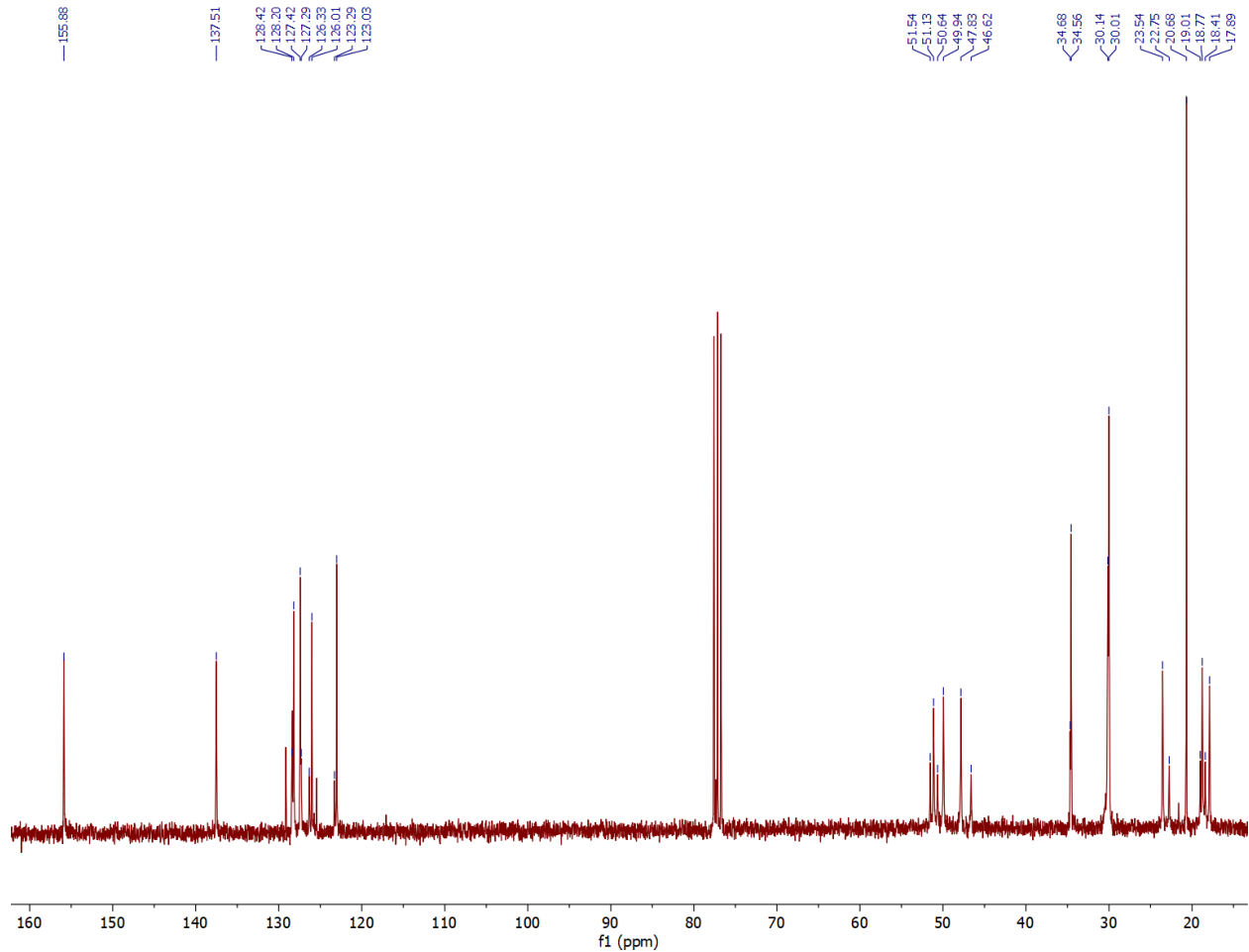


Figure S14. ^{13}C NMR spectrum of **5** in CDCl_3 , 298 K

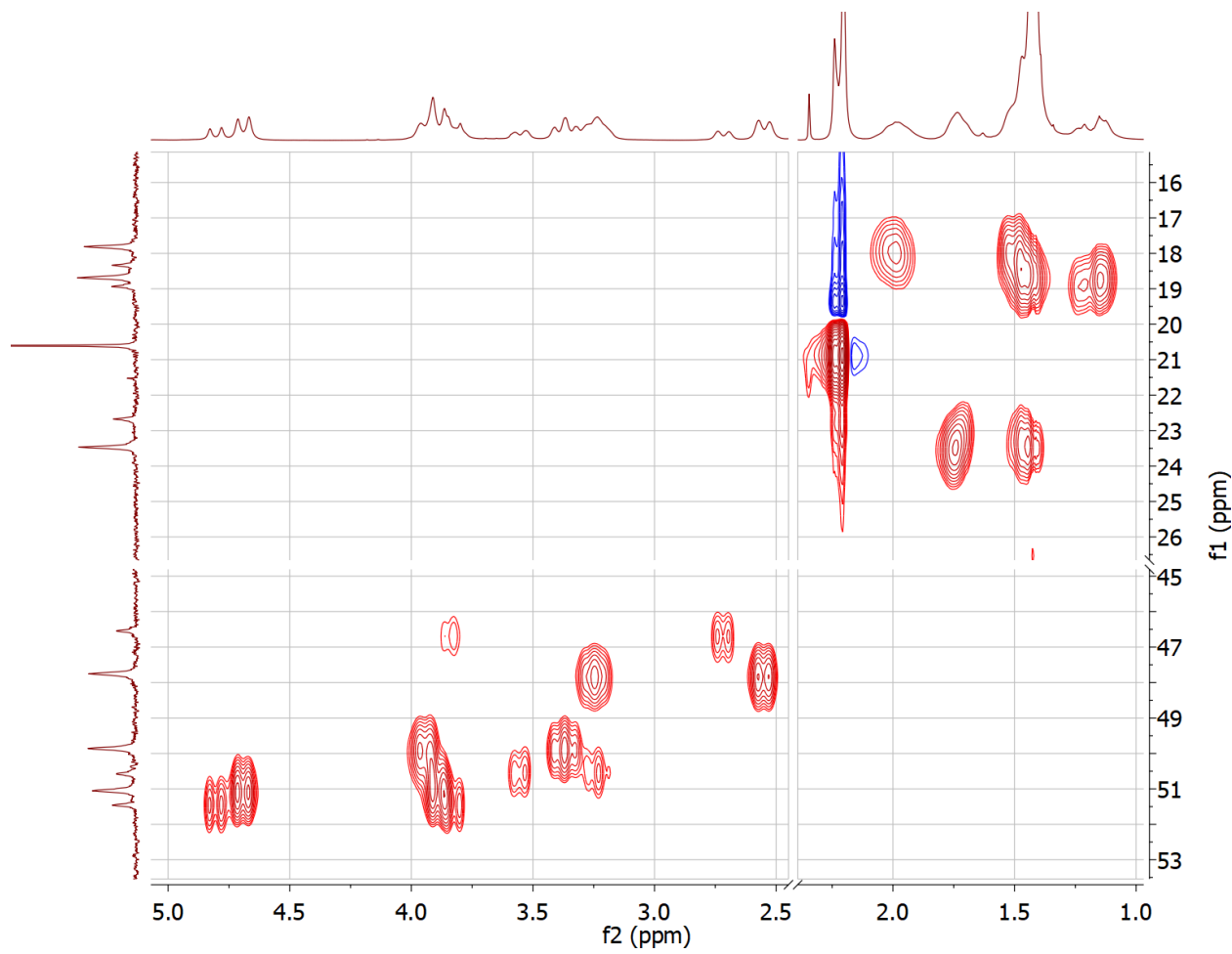


Figure S15. HSQC spectrum of **5** in CDCl_3 , 298 K

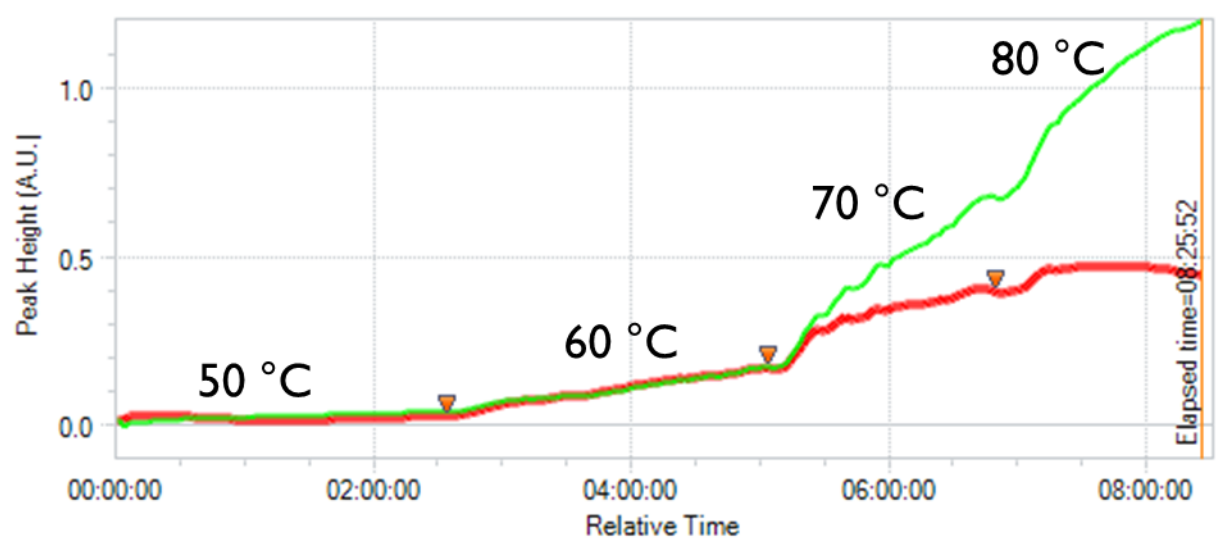


Figure S16. Monitoring of IR absorptions over time at variable temperatures for the reaction of 1+PPNCl+CHO (1/1/500) at 40 bar CO₂. Red (1800 cm⁻¹, CHC formation) and green (1750 cm⁻¹, PCHC formation). Note: Under ideal circumstances, individual and replicant reactions should be performed at each temperature.

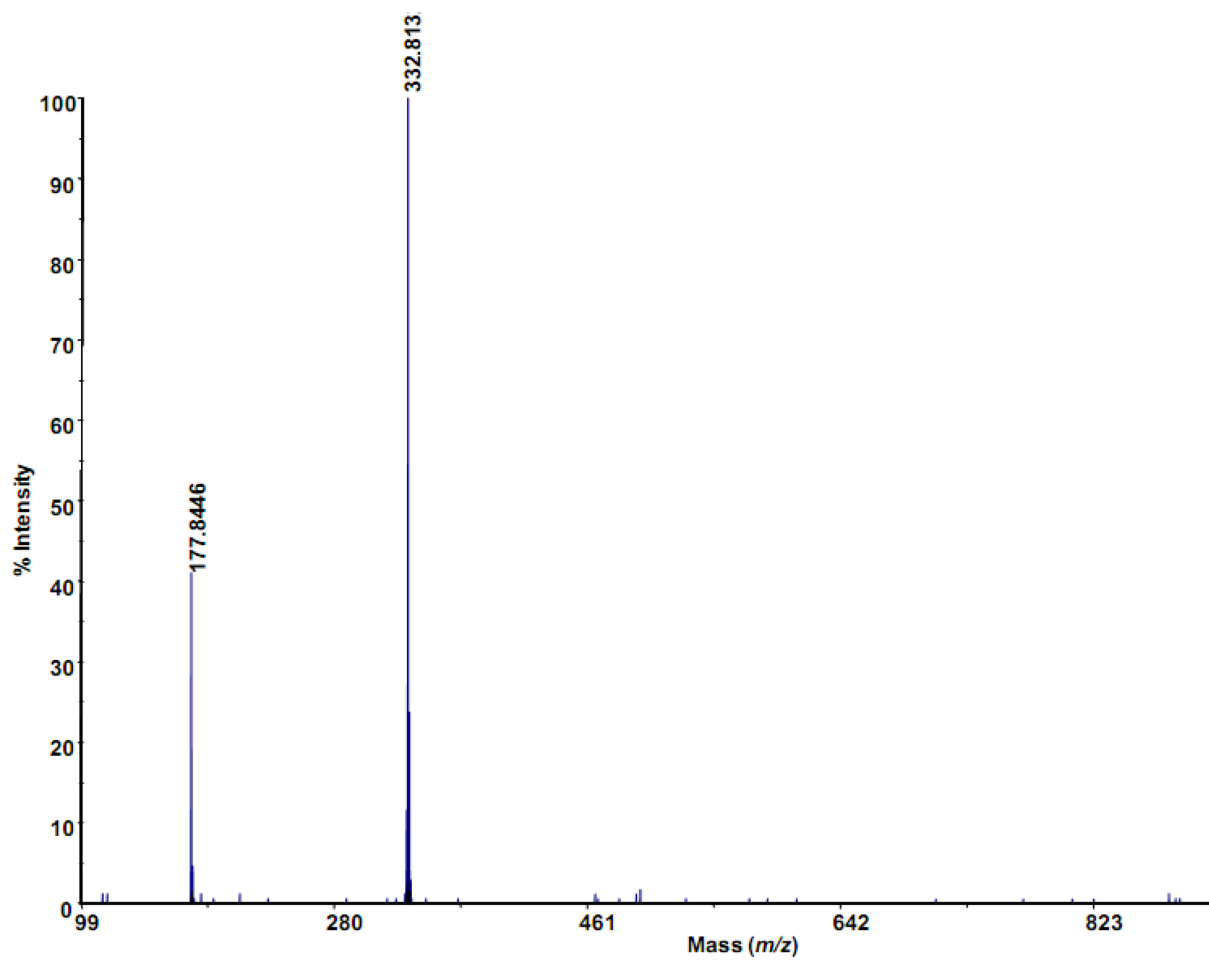


Figure S17. MALDI-TOF mass spectrum of H[L2]

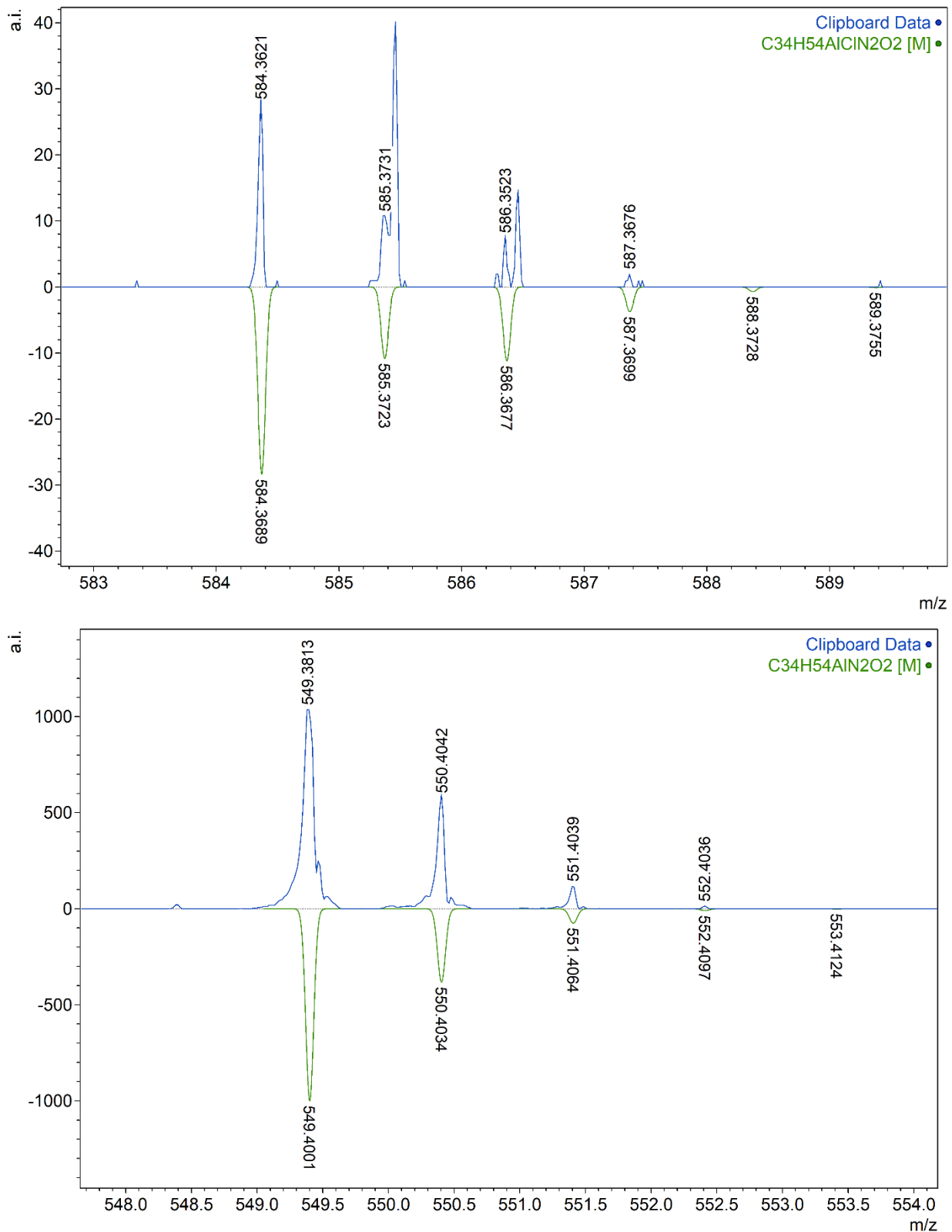


Figure S18. MALDI-TOF MS spectra of **2**

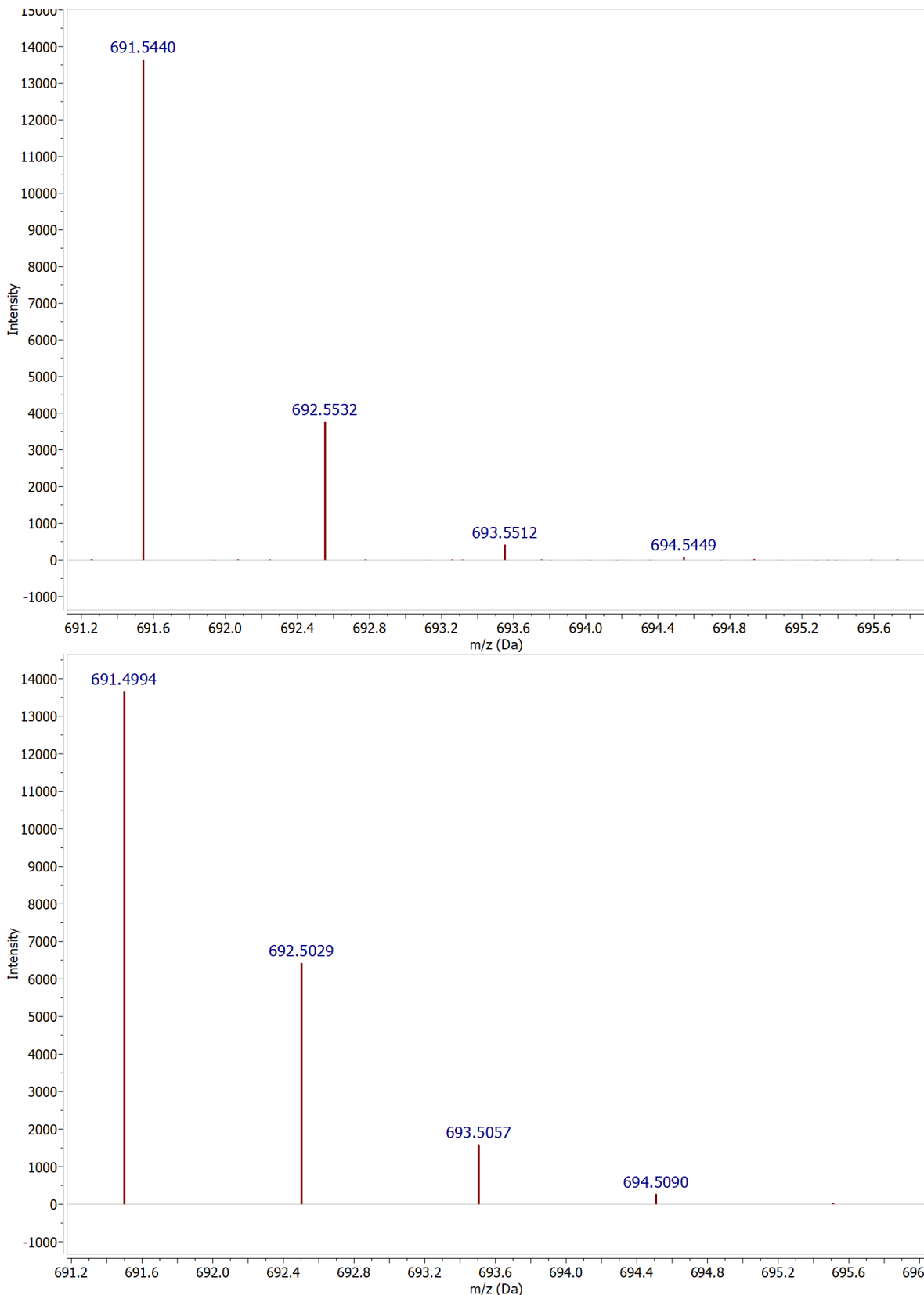


Figure S19. MALDI-TOF mass spectra of **4.3** (experimental – top, theoretical – bottom)

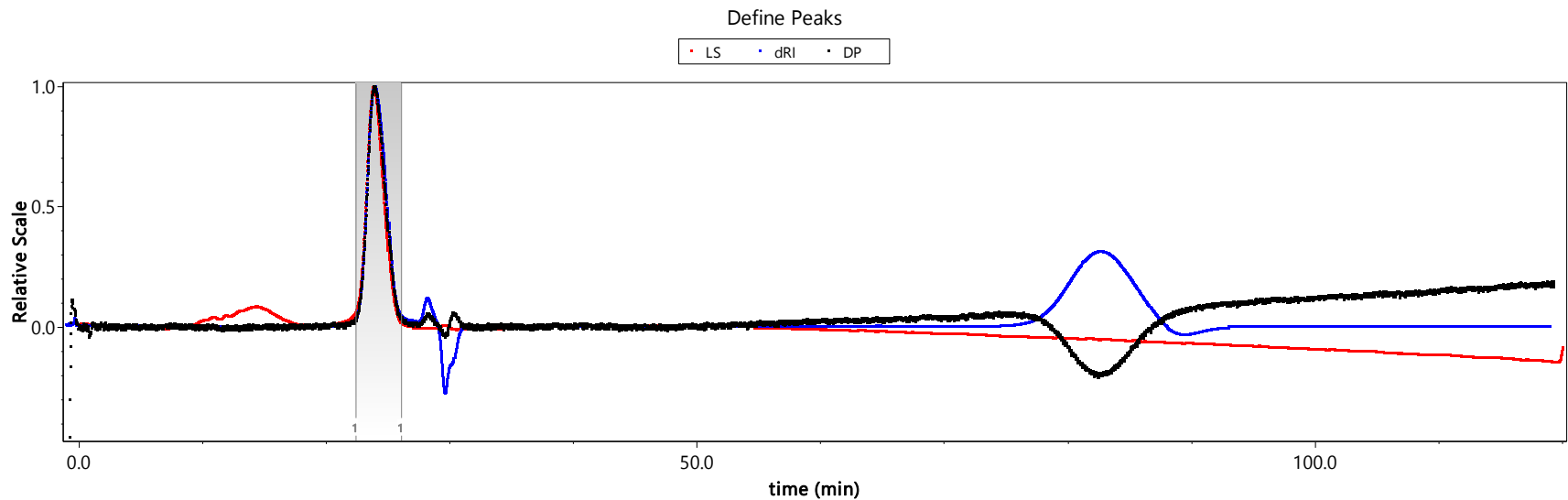


Figure S20. Representative GPC trace of isolated PCHC (Table 1, entry 6; the peaks around 80 min are due to the delay volume)

Table S2. Experimental (X-ray) and calculated (M06/6-311+G(d,p)) bond distances of **1**, **2**, **4**, and **5**

Cat.	Al–O(phenolate) (Å)		Al–N(axial) ^a (Å)		Al–N(pendent) (Å)		Al–Cl (Å)	
	Expt	Calcd	Expt	Calcd	Expt	Calcd	Expt	Calcd
1	1.75	1.77	2.10	2.16	2.08	2.07	2.26	2.28
	1.75	1.77						
2	1.75	1.77	2.12	2.19	2.07	2.06	2.25	2.27
	1.75	1.77						
4	1.77	1.77	2.13	2.13	—	—	2.20	2.20
	1.77	1.77	2.13	2.13				
5	1.77	1.78	2.12	2.15	—	—	2.20	2.20
	1.77	1.78	2.12	2.15				

^a In **4** and **5**, the pendent nitrogen donors also assume axial positions.

Table S3. Calculated charges of pendent nitrogen in initial pro-ligands and Al-Cl complexes

Complex	Mulliken		MSK		CM5		NBO		DDEC6	
	Initial	Al-Cl	Initial	Al-Cl	Initial	Al-Cl	Initial	Al-Cl	Initial	Al-Cl
1	-0.03	-0.97	-0.49	-0.34	-0.39	-0.32	-0.59	-0.66	-0.22	-0.22
2	-0.10	-1.11	-0.28	-0.20	-0.40	-0.32	-0.59	-0.69	-0.16	-0.15

Table S4. Calculated (M06/6-311+G(d,p)) Al charges and relevant bond distances of Al-carbonate derivatives

Cat.	Mulliken	MSK	CM5	NBO	DDEC6	Al–N(pendent) (Å)	Al–carbonate (Å)
1	1.37	1.18	0.48	2.10	1.48	2.08	1.84
2	-0.02	1.12	0.47	2.10	1.48	2.04	1.85
4	-1.69	0.63	0.49	2.18	1.51	2.14, 2.12	1.81
5	-1.69	0.55	0.48	2.18	1.51	2.13, 2.13	1.81

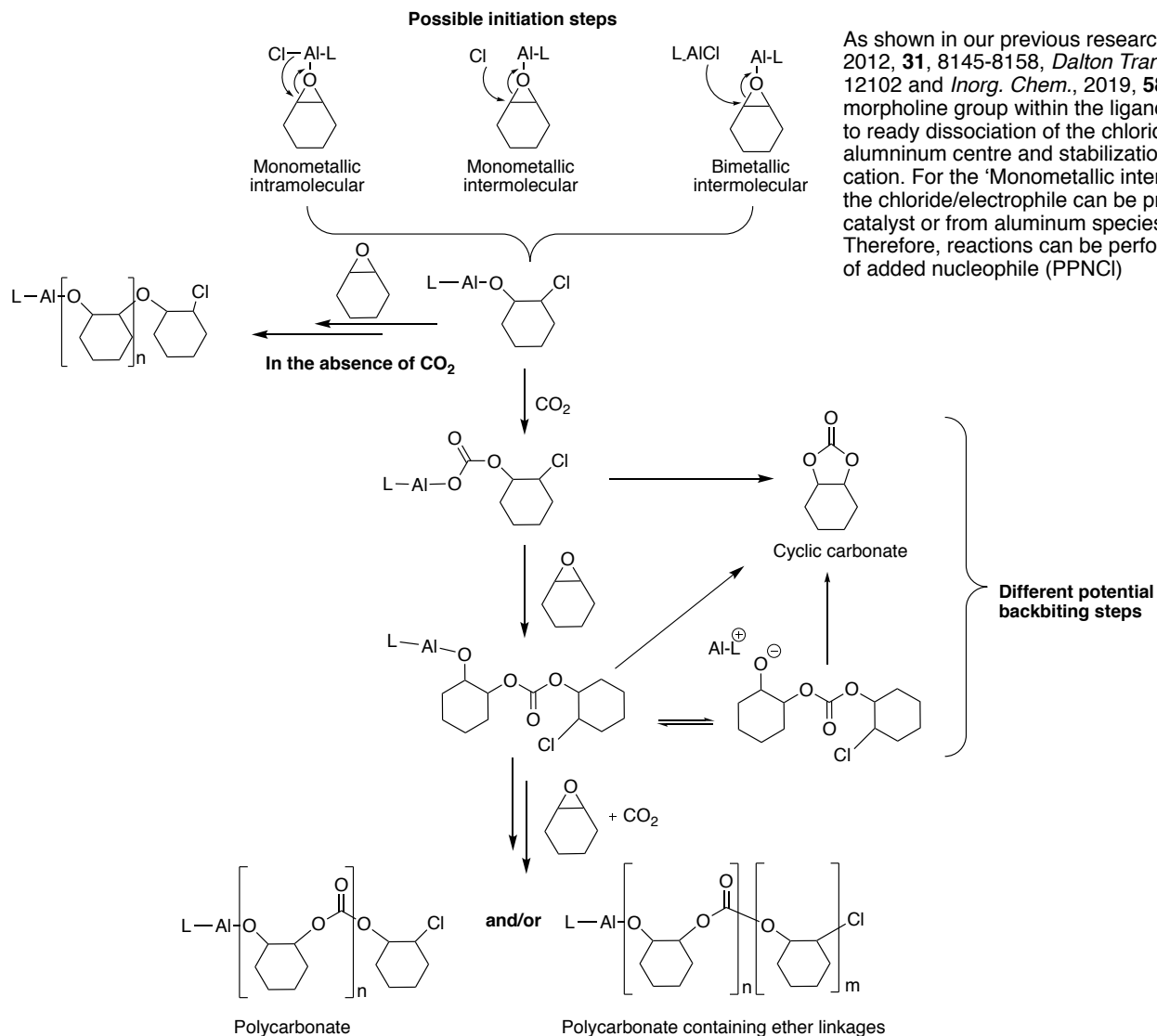
Table S5. Highly active catalyst systems for copolymerization of CHO/CO₂

Entry	Ref	Cat.	Cocat.	T (°C)	P (bar)	% copolymer	TOF (h ⁻¹)
1 ^a	¹	Zn₂	-	100	40	83	85500
2 ^b	²	MgCo	-	140	20	>99	12460
3 ^c	³	Co₂salen	PPNX	25	20	>99	1409

^a 0.025 mol% catalyst ^b 0.05 mol% catalyst ^c 0.1 mol% catalyst, 0.2 mol% PPNX (X = 2,4-dinitrophenoxide)

References

1. S. Kissling, M. W. Lehenmeier, P. T. Altenbuchner, A. Kronast, M. Reiter, P. Deglmann, U. B. Seemann and B. Rieger, *Chem. Commun.*, 2015, **51**, 4579-4582.
2. A. C. Deacy, A. F. R. Kilpatrick, A. Regoutz and C. K. Williams, *Nat. Chem.*, 2020, **12**, 372-380.
3. Y. Liu, W. M. Ren, J. Liu and X. B. Lu, *Angew. Chem. Int. Ed.*, 2013, **52**, 11594-11598.



As shown in our previous research (*Organometallics*, 2012, **31**, 8145-8158, *Dalton Trans.*, 2015, **44**, 12098-12102 and *Inorg. Chem.*, 2019, **58**, 5253-5264), the morpholine group within the ligand framework can lead to ready dissociation of the chloride ligand from the aluminium centre and stabilization of the resulting cation. For the ‘Monometallic intermolecular’ initiation the chloride/electrophile can be present from the co-catalyst or from aluminium species in solution herein. Therefore, reactions can be performed in the absence of added nucleophile (PPNCl)

Figure S21. Possible catalytic mechanisms for ROCOP mediated by Al complexes